European Geothermal Congress 2016

Strasbourg, France, 19-24 Sept 2016

Jolokia EGS – the limits of hydraulic stimulation

Robert Hogarth[1], Stefan Baisch[2], Heinz-Gerd Holl[3], Rob Jeffrey[4], Reinhard Jung[5]

[1] Hogarth Energy Resources, 106 Shorncliffe Pde, Shorncliffe, QLD 4017, Australia

[2] Q-con GmbH, Marktstr 39, D-76887 Bad Bergzabern, Germany

[3] Centre for Coal Seam Gas, University of Queensland, St Lucia, QLD 4072, Australia

[4] SCT Operations Pty Ltd, Cnr Kembla & Beach Streets, Wollongong, NSW 2500, Australia

[5] Jung-Geotherm UG, Gottfried-Buhr-Weg 19, D-30916 Isernhagen, Germany

hogarth.nrg@icloud.com

Keywords: enhanced, geothermal, granite, in-situ stress, fracture, fault, shearing, Habanero, Australia.

ABSTRACT

Geodynamics Limited began developing Enhanced Geothermal Systems (EGS) in hot granite beneath the Cooper Basin in Central Australia in 2002. Successful drilling and stimulation at Habanero lead to drilling of an exploration well, Jolokia 1, located 10 km west of Habanero.

Jolokia 1 penetrated hot granite similar to that encountered at Habanero and reached total depth of 4,911 mRT in 8½" hole without any major drilling issues. The well was completed with a liner set at 4,320 m, leaving 591 metres of open-hole, all in granite.

Preparations for stimulation of the Jolokia open-hole section were based upon experience from Habanero, where injection rates of up to 53 L/s (20 bbl/min) had been reached. However, the stimulation at Jolokia only ever achieved very low injection rates. During most of the stimulation, injection rates averaged 1 L/s (0.4 bbl/min), despite using NaCl brine to increase bottomhole pressures and applying surface pressure of up to 69 MPa (10,000 psi).

A small quantity (21 m^3) of saturated NaBr brine was used to further increase bottomhole pressures, resulting in the injection rate briefly increasing to 7 L/s (2.6 bbl/min). However, injection rates subsequently declined once the dense brine had left the wellbore, returning to rates similar to those before the NaBr stage.

At both Jolokia and Habanero, the granite is known to be in a thrust stress regime, where the minimum principal stress is vertical and where critically stressed fractures, which are prone to shearing, are oriented close to horizontal. At Habanero, stimulation had initiated tens of thousands of micro-seismic events from shearing in a fault zone dipping at 10° from horizontal. During most of the two-week stimulation of Jolokia, estimated bottomhole pressures were greater than the estimated minimum (vertical) principal stress. Even so, at Jolokia, only 234 micro-seismic events were recorded during and after the stimulation. These were clustered into three distinct groups and indicate that the shearing was occurring on three steeply dipping fracture surfaces.

The stimulation rate and pressure history and the micro-seismic data are analysed. A summary of the main conclusions from this unsuccessful attempt to create an Enhanced Geothermal System are provided, along with a discussion of the possible implications for attempts to 'engineer' fractures in unfractured basement rocks.

1. INTRODUCTION

The presence of a potential geothermal energy source near Innamincka in Central Australia was first identified by a petroleum exploration well that encountered hot granite at a depth of 3,748 mRT. Geodynamics Limited (Geodynamics) began exploring the potential for Enhanced Geothermal Systems (EGS) in this hot granite in 2002. Three full-sized wells were drilled at the Habanero location between 2003 and 2008 and a fourth well was drilled in 2012. All these wells have required heavy weight drilling mud (approx. 1,800 kg/m^3) to balance approx.

34 MPa (4,900 psi) overpressures within the sediments above the granite and within the granite. All four of these Habanero wells have recorded various indications of fracturing or faulting within the granite. However, the vast majority of fluid flows, either into or out of the granite, occurred over a short section of intense fracturing now known as the Habanero Fault (Holl, 2015). This structure is interpreted to be a pre-existing thrust fault, dipping at approximately 10° to the west-southwest.

Stimulations of the Habanero Fault have been conducted in three wells: Habanero 1, 3 and 4. In these stimulations, injection rates of up to 53 L/s (20 bbl/min) were achieved and tens of thousands of induced seismic events were recorded. Hypocentre locations of Habanero events align along the pre-existing, sub-horizontal Habanero Fault and extend over an area of 4 km^2 (Baisch et al., 2006; 2009; 2015).

The successful drilling and stimulation at Habanero lead to drilling of an exploration well, Jolokia 1, located 10 km west of Habanero. The well was drilled in 2008 and penetrated hot granite similar to that encountered at Habanero. Again, heavy weight drilling muds were required to balance overpressures. After setting casing in granite at 3,770 mRT, an 8½" hole was drilled to total depth of 4,911 mRT without any major drilling issues. A suite of wireline logs comprising density, neutron porosity, spectral gamma, full waveform sonic and acoustic borehole image were recorded in the open-hole.

The well was completed with a 7" liner set at 4,320 m, leaving 591 metres of open-hole, all of which was in granite. The open-hole section deviated from vertical along an azimuth of 350º, increasing from 14º deviation at the liner shoe to 39º deviation near the toe of the well. Preparations for stimulation of the Jolokia open-hole section were based upon experience from Habanero and the stimulation was conducted in October-November 2010.

2. FRACTURE IDENTIFICATION

Despite using logging tools with high temperature ratings, the combination of high temperatures, borehole breakout and very high mud density resulted in poor quality log data, particularly deeper in the well. Consequently, indications of fracturing from multiple data sources were compared in an effort to obtain consistent fracture identifications (Holl, 2011).

The clearest indication of fractures was obtained from an acoustic formation imaging tool (AFIT). Data was acquired down to 4,590 mRT, but despite the use of a custom-built 'mud excluder' to reduce the impact of the heavy weight mud, data quality is poor. However, 108 fracture indications were identified down to 4,377 mRT. Below this depth the image quality is inadequate for fracture identification. The interpreted fractures are predominantly shallow dipping as shown in an equal-area projection (Figure 1), though some structures dipping 65-85º were identified. It is worth noting though that steeply dipping fractures will be under-represented in a near vertical well.

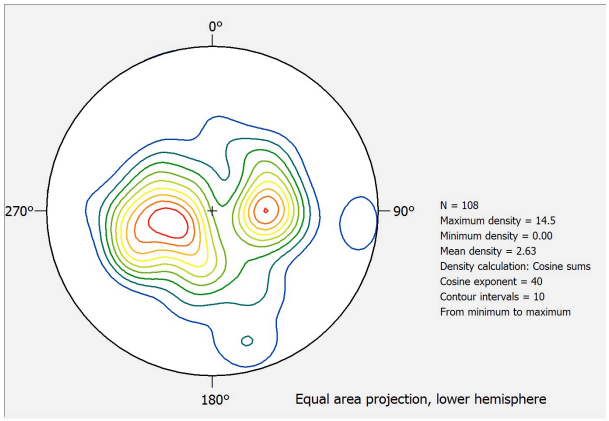

Figure 1: Density stereogram showing clustering of the unfiltered Jolokia fracture data set, corrected for wellbore deviation. Contouring of the poles allow the identification of two shallow dipping maxima. A less distinct steeply North and West dipping population is also shown.

Two fractures were detected by the Managed Pressure Drilling system. The first fracture at 3,822 mRT has been called the 'dog fracture' and flowed into the well at 0.66 L/s (15 bbl/hr). The dog fracture was cemented up and drilling proceeded. A second fracture was detected at 4,065 mRT but was determined to be non-productive and was not cemented (Wyborn, 2009). Both these MPD indications align with fractures identified on the AFIT image.

A cross-dipole full waveform sonic log was recorded down to 4,520 mRT. Unfortunately, the data quality degrades with depth, most probably because of gradual thermal degradation of the wireline cable. The sonic waveforms were presented in a variable density log (VDL) display in which 'chevron patterns' may be associated with fractures intersecting the wellbore. Four good quality chevron patterns were detected on the VDL between 3,785 and 3,940 mRT, all of which align with fracture picks on the AFIT image. Partial chevrons were detected down to 4,100 mRT but below this depth the data quality is too poor for identification of chevrons.

The sonic log data was also used for Stoneley wave analysis, which again seeks to identify fractures intersecting the borehole (Castillo, 2009). Unfortunately, the Stoneley wave analysis is also affected by degrading data quality, though in this case the result is an unrealistic increasing indication of fracturing with depth.

For the deeper section of the hole, the only data sources available are mechanical drilling parameters

(DP) and density, neutron porosity and spectral gamma ray logs. The drilling parameters, such as rate of penetration, weight on bit and torque, were used to infer mechanical heterogeneities within the granite, which could be fracture related or simply caused by changes of rock type (e.g. aplite injections). These indications were compared with gas readings (mainly CO_2) from the drilling mud and references in the cuttings analysis to alteration zones that could be indicative of fracture mineralization.

A comparison of the fracture indications from the drilling parameters (DP), the VDL chevron pattern analysis, the Stoneley wave analysis (XMAC) and the image log (AFIT) is shown in Figure 2. The DP, VDL and AFIT bars are quality related whilst the XMAC bars are frequency related.

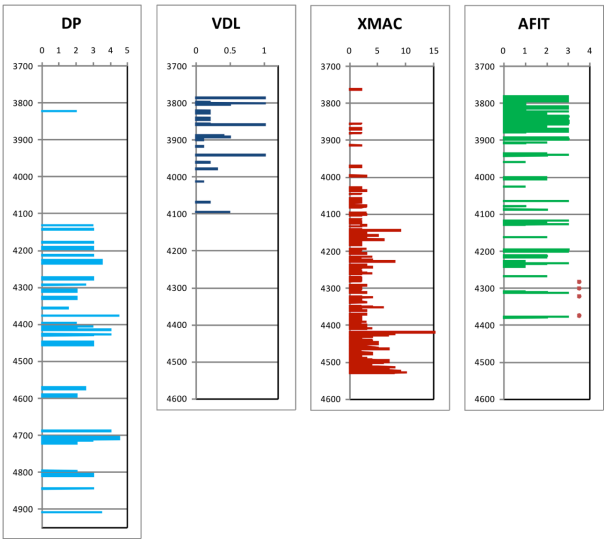

Figure 2: Comparison of fracture indications from drilling parameter analysis (DP), chevron pattern analysis (VDL), Stoneley wave analysis (XMAC), and the picked fractures from the image log (AFIT). Vertical axis shows the depth in mRT. Bar width is quality linked. The widest bars are related to best quality.

The density and neutron porosity log data is strongly affected by borehole breakout, some of which may be related to fracturing. Two zones showing significant breakout were identified at around 4,375 and 4,700 mRT. The shallower of these aligns with the deepest fracture pick on the AFIT and the deeper of these aligns with a cluster of mechanical heterogeneities from the drilling parameters.

On the basis of these limited indications of fractures in the deeper section, a 7" liner was set at 4,320 mRT, leaving 591 metres of open-hole, all of which was in granite.

3. IN-SITU STRESS

The state of stress at Habanero has been determined from wireline logs and drilling data analysis (Barton et al., 2013). This stress magnitude analysis clearly indicates a strike-slip regime in the shallower sediments, changing into a reverse faulting or thrust regime at reservoir depth. The azimuth of the maximum horizontal stress, S_{Hmax}, which is also the maximum principal stress, is 82 ± 5° at reservoir depth as derived from image log analysis of the Habanero wells (Holl and Barton, 2015). The stress regime in the granite section of Jolokia is analogous with the situation at Habanero (thrust). Estimated in-situ stresses at two selected depths in the open-hole section of Jolokia 1 are presented in Table 1. At Jolokia the orientation of S_{Hmax} was determined from the AFIT image log data to be an azimuth of 86 ± 7°.

Depth (mRT)	S_v (MPa)	S_{hmin} (MPa)	S_{Hmax} (MPa)	Pore Pressure (MPa)
4370	103	118	155	75
4500	106	122	160	76

Table 1: Estimated in-situ stress magnitudes at selected depths in Jolokia-1, using a stress ratio of S_{Hmax}:S_{hmin}:S_v of (1.51:1.15:1.0).

4. TEST PERFORMANCE

Various hydraulic and stimulation tests were performed on the open-hole section of Jolokia 1. The major objective of the tests was to stimulate or to create fractures in the granite. The frac-fluid used was a saturated NaCl solution (1,200 kg/m^3). A total volume of about 550 m^3 was injected during the 14 days of the test series. Even though the wellhead pressure was kept at its technical limit of 69 MPa (10,000 psi) over prolonged time-periods, only very low injection rates of around 1 L/s were achieved (Figure 3). In order to achieve higher flow rates and to accelerate the stimulation process, about 21 m^3 of a saturated NaBr solution (1,440 kg/m^3) was injected during the final part of the test series. Several shut-in periods were performed at different stages of the test series in order to obtain information on the evolution of the fracture properties, with emphasis on fracture conductivity (transmissivity) and fracture width.

Prior to stimulation, an influx test and a leak-off test were conducted in order to determine the virgin permeability of the granite and the pressure level for the onset of shearing of pre-existing fractures in the open-hole section.

The influx was induced by controlled venting of fluid via a choke valve in the surface production line. Influx was stopped when pressure depletion of 12 MPa was reached and the pressure build-up recorded for about 1 hour (Figure 4).

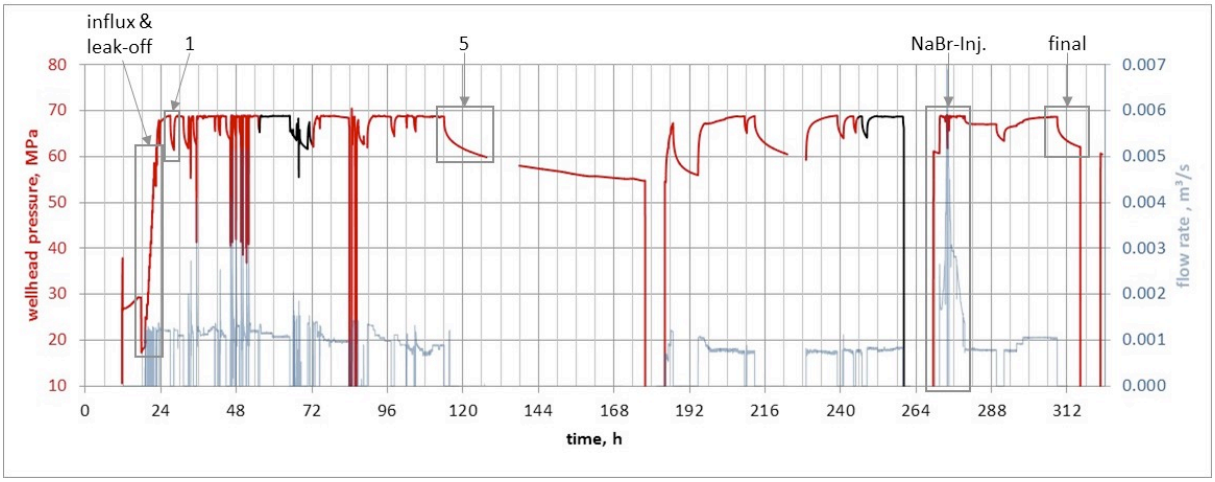

Figure 3: Records of the wellhead pressure (red) and the flow rate (blue) of the hydraulic test series. The test sections analysed below are marked by the grey boxes.

During the leak-off test the pressure was increased in steps by injecting small quantities of saturated NaCl solution at rates of about 1.3 L/s. After each step the borehole was shut-in and the pressure decay recorded (Figure 4). Thirteen steps were performed in this way.

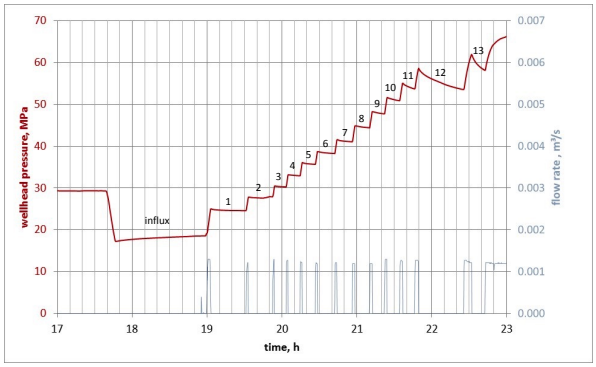

Figure 4: Records of the wellhead pressure (red line) and the flow rate (blue line) of the influx and the leak-off test.

5. TEST ANALYSIS AND RESULTS

The pressure build-up during the influx test followed an almost perfect straight line when plotted over the square root of time and is well matched by a model of linear fracture flow with wellbore storage and no skin (Figure 5). The determined well bore storage coefficient, $Cw = 3.5 \cdot 10^{-8} \pm 0.1$ m³/Pa, fits exactly with the theoretical value for the borehole volume. This excludes the application of a formation linear flow model, which also shows square root of time behaviour. Since the square root of time behaviour persists until the end of the influx-test, the test yields no information on formation permeability. Using a radial flow-model as a proxy, a commercial well test analysis program delivered a permeability value of $k < 5 \cdot 10^{-22}$ m² (< 0.5 nD). This very low value can be regarded only as an "apparent" value. The undisturbed formation pressure cannot be derived from the influx test or from any other part of the test series including the period before the influx-test.

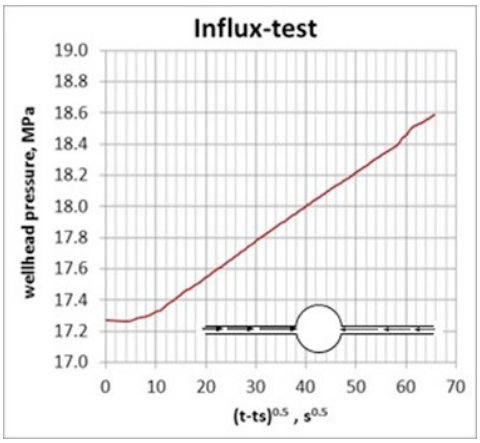

Figure 5: Wellhead pressure record of the influx test plotted vs. the square root of time. t_s: time of shut-in.

The fracture linear flow-model with wellbore storage was applied also to evaluate the leak off test. Because of the expected pressure dependency, each step was treated separately and corrected for the trend resulting from the preceding step (Jung, 2010). The transmissivity values obtained in this way are plotted as a function of the wellhead pressure at shut-in (Figure 6, upper). Fracture transmissivity shows a slight but distinct increase with pressure even at low wellhead pressure. This may be attributed to elastic widening of the fracture(s). At about 50 MPa fracture opening accelerates dramatically indicating the onset of shearing.

Fracture width was determined from fracture transmissivity by using the cubic law:

$$T_f = 12\, w_f^3 \qquad [1]$$

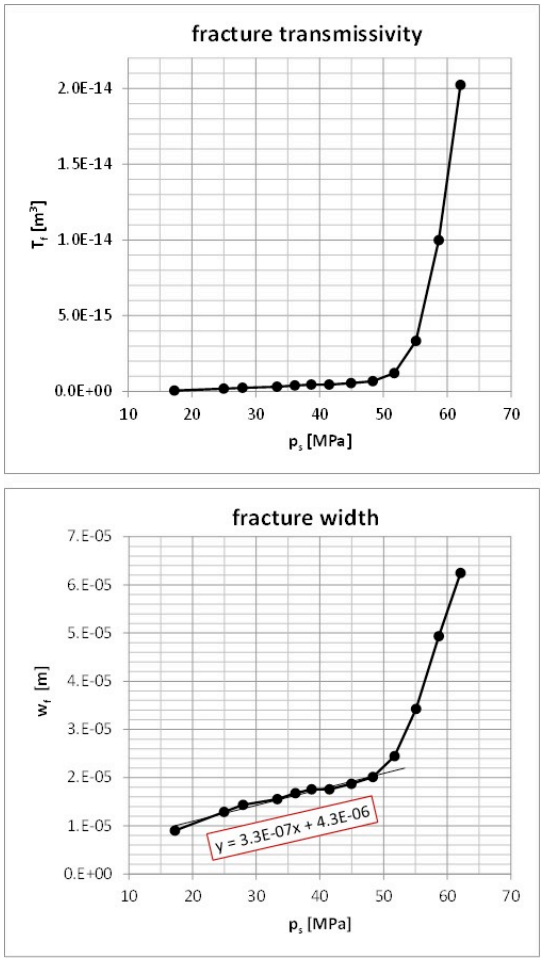

Figure 6: Fracture width and fracture transmissivity determined from the influx and leak-off tests (assuming fracture height 100 m) vs. wellhead pressure p_s at shut-in. The fit line in the lower diagram yields the fracture storage coefficient.

A diagram of fracture width versus pressure (Figure 6, lower) exhibits two almost linear intervals, with a small slope below 50 MPa wellhead pressure and a much higher slope above 50 MPa. Assuming purely elastic widening of the fracture in the low pressure range, the slope of this straight line section is identical with the storage coefficient of the fracture, $S_f = dw_f/dp$. This value however is generally not identical with the estimated value used for the determination of fracture transmissivity and hence fracture widths, but by iteration the "true" value of $S_f = 3.3 \cdot 10^{-13}$ m/Pa was determined. The same value was applied for determining the transmissivity in the high-pressure regime assuming that the fracture storage coefficient is only weakly pressure dependent.

In contrast to the influx and the leak-off tests, the later shut-in periods showed a distinct bilinear flow behaviour characterized by a pressure decline proportional to the fourth root of time (Figure 7). It is well known that the fracture linear flow period turns into the bilinear flow period after a certain time provided the fracture is sufficiently long (e.g. Ortiz et al., 2013). When this happens, fluid loss into the rock becomes more important than fluid storage within the fracture and permeability and storage coefficient of the rock instead of the fracture storage coefficient have to be known or assumed for determining fracture

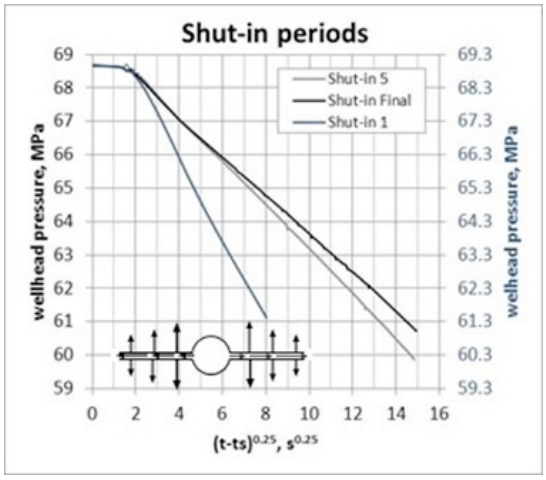

Figure 7: Wellhead pressure records of shut-in periods 1, 5 and final vs. the fourth root of time. t_s: time of shut-in.

transmissivity and width from the slope of the fourth root straight lines of Figure 7. Through iteration, reasonable values for both parameters were determined making the transmissivity values of the shut-in periods compatible with the trend of the fracture widths of the leak-off test.

The diagram of the wellhead pressure versus fracture width summarizes the results of the hydraulic analysis in an illustrative manner (Figure 8).

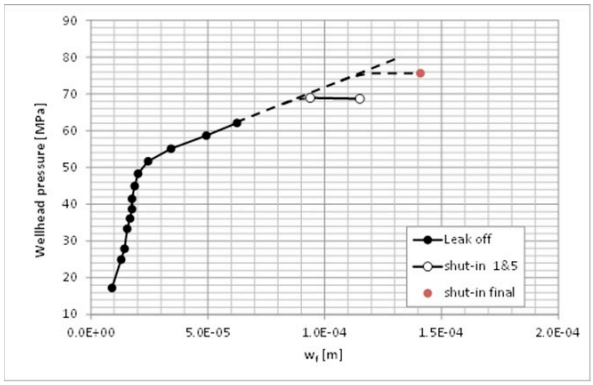

Figure 8: Wellhead pressure (at shut-in) vs. fracture width (assuming fracture height 100 m). The pressure value for the final shut-in is virtual. It corresponds with the downhole pressure increase during NaBr-brine injection.

Fracture opening in the initial part below 50 MPa occurs in a normal mode due to the unloading of the

asperities within the fracture. At 50 MPa shear movement starts and fracture width increases due to the movement of the two fracture surfaces on surface irregularities. For the very short injection periods of the leak-off test the data points are on a straight line and it is reasonable to assume that additional data points obtained in the same manner would also follow this line at higher pressure (dashed line in Figure 8). When larger fluid volumes are injected at constant pressure, fracture width is increasing with time or injected volume (see data points for shut-in periods 1 and 5 in Figure 7).

This effect is explained by assuming that the front of the shear zone is migrating further away from the borehole giving room for additional shear movements in the centre part. At the surface pressure level of 69 MPa (corresponding to a pressure of 116 MPa at 4370 mRT) this process consumed only a moderate flow rate (about 1 L/s). Accordingly, the shear-front migrated slowly. When the bottomhole pressure was raised by some 6 MPa as was done during the NaBr injection period, the migration speed of the shear front accelerated and a much higher flow-rate was consumed and fracture width and conductivity increased further (see data point of the final shut-in period in Figure 8).

6. INDUCED SEISMICITY

Stimulation activities were monitored with a 17-element seismic monitoring network consisting of surface seismometers and geophones deployed in shallow boreholes at depth levels of approx. 100 m (Baisch et al., 2015).

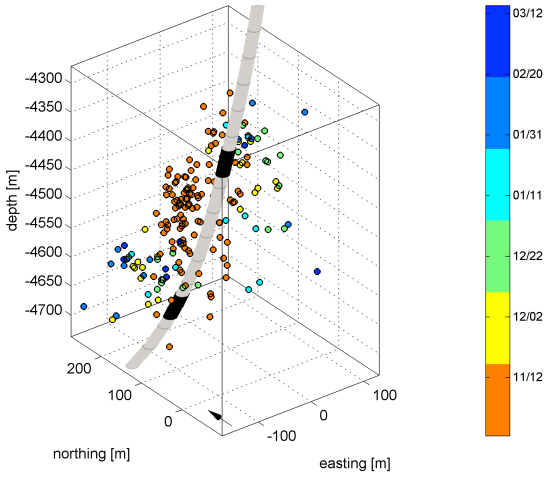

Figure 9: Absolute hypocentre locations in perspective view looking from the southwest. Colour encoding denotes origin time. A total of 182 located events are shown. Coordinates are given in meters with respect to the wellhead. The grey line shows the well trajectory. Likely fracture intersections are indicated in black.

During the 14 days stimulation period, a total of 73 events were detected. The first seismic event was detected whilst pumping at a surface pressure of 69 MPa (bottomhole pressure 116 MPa). Event magnitudes determined relative to the magnitude scale described by Baisch et al. (2009) range between M_L=-1.4 and M_L=1.0. Another 139 events occurred within the following 6 months, with the strongest event (M_L=1.6) occurring 127 days after the injection was terminated.

Figure 9 shows the resulting hypocenter distribution. Average location errors on a 2σ confidence level are 52, 54, and 80 m into the eastern, northern, and vertical direction, respectively. Seismic events tightly cluster along a vertically elongated structure following the trajectory of the Jolokia well. Most events are located within 100 m lateral distance from the wellbore trajectory.

Based on their waveform similarity, events can be grouped into three clusters (Baisch et al., 2015). Fault plane solutions (Figure 10) are extremely similar for events belonging to the same cluster. The best fitting solution for the largest cluster family (Figure 10, a) indicates a strike-slip mechanism on a steeply dipping plane. This is approximately consistent with the orientation of the planar distribution of relative hypocentre locations (Baisch et al., 2015). The best fitting fault plane solutions for the other two clusters are compatible with oblique faulting with a thrust faulting component.

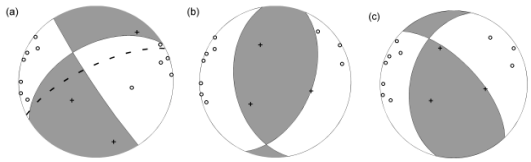

Figure 10: Best-fitting fault-plane solutions (beachballs) of typical events belonging to the three event clusters determined by Baisch et al. (2015). Dashed line in (a) indicates the orientation of the fault plane as outlined by relative hypocenter locations.

The orientation of these fault plane solutions for the three event clusters is very similar to the orientation of steeply dipping fractures observed on the acoustic borehole image (Figure 11). This suggests that the structures that are shearing are pre-existing natural fractures.

Compared to Habanero stimulations where tens of thousands of micro-seismic events were detected, the stimulation of Jolokia caused only minor seismic activity. Hypocentres are located in the immediate vicinity of the Jolokia well and align along steeply dipping fractures which are not well oriented for shearing in the regional stress-field. These findings indicate that the availability of hydraulically

conductive fractures plays a critical role for the stimulation of enhanced geothermal system reservoirs.

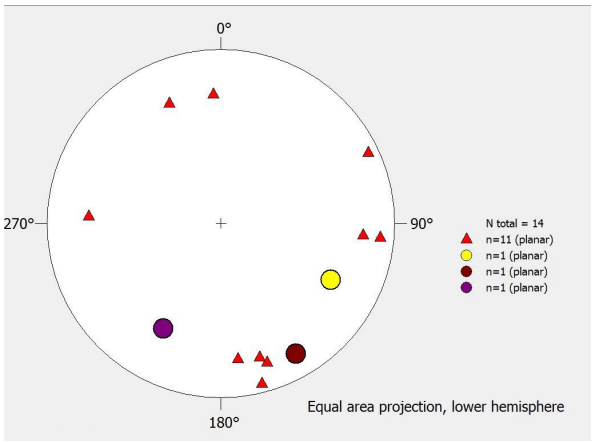

Figure 11 – Stereonet showing all steeply dipping fractures from the acoustic borehole image (triangles) and the best-fitting fault plane solutions for the three clusters of seismic events (circles).

7. BOTTOMHOLE PRESSURE AND BREAKDOWN

During the stimulation, pressure and injection rate were recorded at the surface. The bottomhole pressure was calculated based on adding a hydrostatic component, arising from the elevation difference and fluid density, and subtracting the pressure loss from fluid viscous friction in the well. The depth location of the displacement front between the NaBr and NaCl brines was calculated and fluid densities that accounted for the effects of pressure and temperature were used in the bottomhole pressure calculation.

Because of the well completion design, the surface pressure at the well head was limited to not exceed 69 MPa (10,000 psi). The predominant natural fractures were sub-horizontal (Figure 1) but based on the well response did not provide a weakness for initiation of a horizontal opening mode hydraulic fracture at the wellbore. The in-situ stress conditions given in Table 1 favour growth of horizontally oriented fractures if pressures sufficient to propagate opening mode hydraulic fractures are used.

Figure 12 shows the surface pressure and surface injection rate together with the calculated bottomhole pressure for the period of time during which the heavy NaBr brine was injected. Just prior to the start of NaBr, the bottomhole pressure was calculated to be 116 MPa during injection of NaCl. The calculated bottomhole pressure increased to a maximum of 122 MPa when the NaBr had been completely injected. The vertical stress was estimated as 103 MPa, with all these pressures at a reference depth of 4370 mRT. There is only a small drop in pressure immediately upon shut-in, and the small compressible flow effects would not have produced significant after flow upon shut-in to affect the pressure drop. Less than 1 MPa of near well entry pressure loss are present in the data shown in Figure 12.

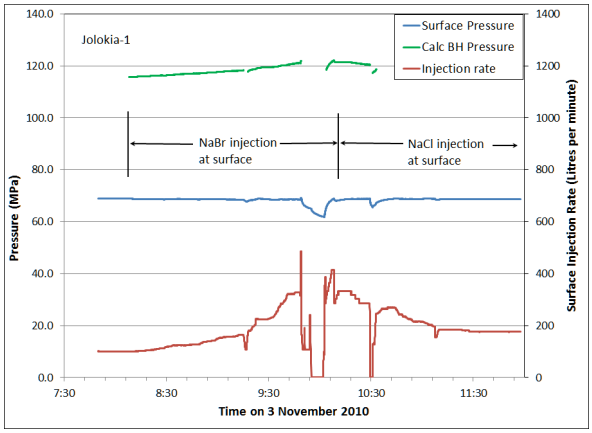

Figure 12 - The blue line is the measured surface pressure, the green line is the calculated bottomhole pressure at 4370 m during the NaBr injection stage. The corresponding injection rate, measured at the surface, is given by the red line. Approximately half the well was eventually displaced to NaBr brine before switching back to NaCl brine.

During injection of the NaCl brine, the surface pressure was near 69 MPa (116 MPa bottomhole), which is above the vertical stress magnitude of 103 MPa at 4370 mRT, but below the pressure required to breakdown the wellbore by axial or sub-axial splitting. An axial wellbore breakdown in opening mode would produce a vertical fracture that would rapidly reorient to a horizontal plane (Jeffrey et al., 2012). Such initiation and reorientation is associated with the development of significant tortuosity in the fracture path near the wellbore, resulting in high pressure from near-wellbore fracture entry losses (Jeffrey et al., 2015).

A rate versus pressure plot for the period of NaBr brine injection shows an inflection at 119 MPa bottomhole pressure (Figure 13) that is consistent with initiation of a hydraulic fracture and the beginning of such a breakdown process. Perhaps because of the development of tortuosity during this initial fracture growth period, a declining pressure with time response, which is normally associated with opening mode fracture development, did not develop. All of the available NaBr brine was injected and the bottomhole pressure decreased to 116 MPa once NaCl brine was resumed, before the breakdown process could be completed.

As shown in Figure 13, stress conditions listed in Table 1 are such that a pressure in the borehole of less than 119 MPa is insufficient to initiate a new axial fracture or even open an existing vertical fracture unless it were perfectly aligned with the maximum horizontal stress direction. Thus it seems an

explanation for the observed pressure and rate response during the NaCl injection period is that a number of sub-vertical natural fractures were pressurised below their opening pressure, but were dilated by the pressure and by shearing, as shown by the data in Figures 6 and 8.

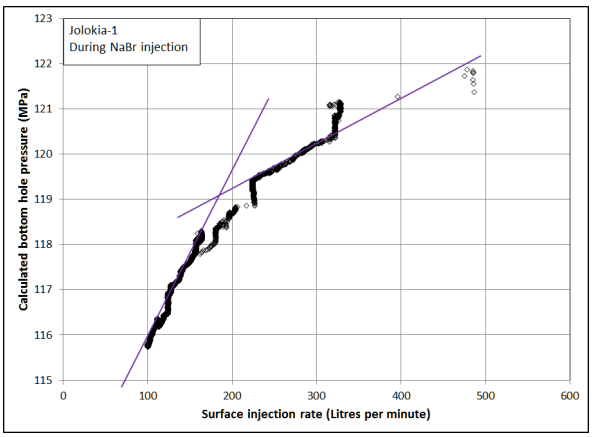

Figure 13: Injection rate versus calculated bottomhole pressure at 4370 mRT during the injection of 21 m^3 of NaBr brine. The change in slope that occurs at approximately 119 MPa is indicative of initiation of an opening mode hydraulic fracture.

The scenario that precludes growth of a sub-vertical opening mode fracture, except for a short time during injection of the NaBr brine, and instead relies on the injected fluid entering dilating natural fractures is more consistent with the pressure and rate data recorded.

8. CONCLUSIONS

Of the data sets used to try to detect fractures in the granite, the acoustic borehole image provided the most reliable results.

The acoustic borehole image shows the presence of both fractures that are shallow dipping and fractures that are steeply dipping.

In the thrust stress regime present in the granite at Jolokia, shallow dipping fractures striking approximately North-South would be optimally oriented for shearing. Fractures with this orientation were common in the acoustic borehole image.

The micro-seismic data indicates shearing on at least three distinct, steeply dipping fault planes.

The orientations of these three fault planes are similar to orientations of steeply dipping, naturally occurring fractures detected from acoustic borehole images, suggesting that the shearing has occurred on natural fractures.

Pressures below 97 MPa at 4370 mRT (50 MPa at surface) caused no seismicity and only slight increase in fracture transmissivity, suggesting only elastic dilation of the natural fractures.

Pressures above 97 MPa at 4370 mRT (50 MPa at surface) caused significant increase in fracture transmissivity (20 fold during short-term and another 15 fold during long-term injections), suggesting shearing of the fractures. The first seismic event was detected after injecting about 20 m³ of NaCl brine at a bottom hole pressure of 116 MPa.

Despite applying bottomhole pressures greater than the vertical least principal stress for several days, there was no indication of any shearing on optimally oriented sub-horizontal fractures. This suggests that those sub-horizontal fractures that are present are closed and fully cemented.

Increasing the bottomhole pressure to above 119 MPa by injecting NaBr brine at surface caused a significant increase in injectivity. This is interpreted to indicate the initiation of axial wellbore breakdown in opening mode. This would have created a vertical fracture, aligned with the borehole orientation.

With the limited volume of NaBr brine available, complete opening mode breakdown was not achieved. As bottomhole pressures declined, the vertical fracture closed again.

9. IMPLICATIONS FOR EGS

From the observations at Jolokia one can conclude that:

- Wherever possible, Enhanced Geothermal System developments should target open, hydraulically-conductive fractures or faults that are optimally oriented for shearing in the local stress regime;
- In the absence of open, hydraulically-conductive fractures or faults, creation or engineering of new, opening mode fractures in high-strength, competent rock will likely require very high downhole stimulation pressures and/or other mechanical measures for facilitating fracture initiation.
- Delivery of these high downhole stimulation pressures will require careful design and specification of wellhead and completion equipment.

REFERENCES

Baisch, S., Weidler, R., Vörös, R., Wyborn, D. and DeGraaf, L., 2006: Induced seismicity during the stimulation of a geothermal HFR reservoir in the Cooper Basin (Australia). *Bull. Seism. Soc. Amer.*, 96 (6), 2242-2256.

Baisch, S., Vörös, R., Weidler, R. and Wyborn, D., 2009: Investigation of Fault Mechanisms during Geothermal Reservoir Stimulation Experiments in the Cooper Basin (Australia). *Bull. Seism. Soc. Amer.*, 99 (1), 148-158.

Baisch, S., Rothert, E., Stang, H., Vörös, R., Koch, C. and McMahon, A., 2015: Continued geothermal reservoir stimulation experiments in the Cooper Basin (Australia). *Bull. Seism. Soc. Amer.*, 105, 198-209.

Barton, C., Moos, D., Hartley, L. Baxter, S., Foulquier, L., Holl, H. and Hogarth, R., 2013: Geomechanically coupled simulation of flow in fractured reservoirs. *Proceedings, 38th Workshop on Geothermal Reservoir Engineering,* Stanford University, Stanford, CA (2013), SGP-TR-198.

Castillo, D., 2009: Review of XMAC observations in the Jolokia-1 well and natural fracture detection concepts. Unpublished GMI report to Geodynamics.

Holl, H., 2011: Jolokia 1 Fracture Interpretation – Fracture indications from image logs, XMAC measurements and drilling parameters. Unpublished Geodynamics Limited report.

Holl, H., 2015: What did we learn about EGS in the Cooper Basin? – unpublished Geodynamics Limited report.

Holl, H. and Barton, C., 2015: Habanero Field – Structure and State of Stress. *Proceedings World Geothermal Congress 2015*, Melbourne, Australia.

Jeffrey, R.G, Chen, Z.R., Zhang, X., Bunger, A.P. and Mills, K.W., 2015: Measurement and Analysis of Full-Scale Hydraulic Fracture Initiation and Reorientation. *Rock Mechanics and Rock Engineering*, September 2015, 16.

Jeffrey, R.G., Wu, B., Xi Zhang, Xavier Choi, Bisheng Wu, and Baotang Shen, 2012: An Analysis of the Stimulation of Jolokia-1 carried out during October and November 2010." *Confidential Report EP12064*. CSIRO, January 2012.

Jung, R., 2010: Analysis of pressure decline of three shut-in periods, Jolokia 1, Stimulation test series Oct/Nov. 2010. *Unpublished report Geodynamics Limited*.

Jung, R., 2011: Analysis of the leak-off test, Jolokia 1, Stimulation test series Oct./Nov. 2010. *Unpublished report to Geodynamics Limited*.

Ortiz, A.E., Jung, R. and Renner, J., 2013: Two – dimensional numerical investigation on the termination of bilinear flow in fractures. Solid Earth, 4, 331-345.

Wyborn, D., 2009: Overall development logic for J1 and J2 doublet. *Unpublished Geodynamics report*.

Acknowledgements

We would like to thank Geodynamics Limited for access to the Jolokia data and for allowing us to publish this study. We gratefully acknowledge comments from Friederike Grasse, which helped to improve the final manuscript.